

FINAL REPORT

“Interactions Forces and the Flow-Induced Coalescence of Drops and Bubbles”

Award # NAG3-2115

L. Gary Leal, PI

J. Israelachvili, Co-PI

MACROSCOPIC COALESCENCE STUDIES: FOUR-ROLL MILL EXPERIMENTS AND THEORY

In order to accomplish the proposed macroscale experimental goals, we designed and built a pair of miniaturized computer-controlled four-roll mills, similar but much smaller than the 4-roll mill that had been developed earlier in Prof. Leal's group for studies of drop deformation and breakup.¹⁴ This unique experimental facility allows for controlled experiments on the breakup and coalescence of very small drops in the size range of 20-200 μm in diameter for a wide variety of flows and under a wide range of flow conditions including time-dependent flows, etc. The small size of this device is necessary for coalescence studies, since coalescence occurs in viscous fluids at capillary numbers that are large enough to be experimentally accessible only for drops that are smaller than approximately 100 μm in diameter. Using these miniaturized 4-roll mills, we have obtained the first quantitative data (so far as we are aware) on the flow-induced coalescence process, as summarized below.

(1) **Coalescence Studies with no Surfactant.** Over the past several years, we have utilized NASA support to complete the major portions of a comprehensive experimental study of flow-induced coalescence between two equal size Newtonian drops in a series of different types of steady, linear flow in the 4-roll mill.^{9,10} Although the majority of these experiments were carried out using a combination of modest MW (Newtonian) polymers, experiments were also performed for much lower MW fluids to verify the lack of any measurable dependence on MW.¹⁵ These experiments covered drop sizes from approximately 20 to 200 microns in diameter, a spectrum of different flow types, a range of capillary numbers from approximately 0.0001 to 0.1, and a full range of droplet trajectories ranging from zero offset (i.e., *head-on collisions* which required the development of an additional control scheme to stabilize the orientation of the pair of colliding drops)¹⁵ to *glancing* configurations (i.e., arbitrary initial offset values). For head-on collisions, coalescence must eventually occur for all capillary numbers, and the experimental data of primary interest is the film drainage time (or collision time) from initial 'contact' to coalescence, as a function of drop size, viscosity ratio and capillary number. For glancing collisions with a *finite initial offset* of the centers of the drops from a head-on collision trajectory, the available film drainage time is limited before the drops rotate to the point where they begin to separate in the flow. In this case, coalescence only occurs if the film thins (at least locally) to a sufficient degree that non-hydrodynamic attractive forces are able to destabilize it, leading to rupture. This is favored by 'gentle' collisions, and the key experimental data is then the critical capillary number *below* which coalescence occurs, as a function of the viscosity ratio, drop size, flow type, and most importantly the offset.

Finally, for reasons that will become apparent below, a significant effort was made to quantify the details of the droplet trajectories during the coalescence process. The most important and surprising data was found to be the *coalescence angle* between droplet centers corresponding to the critical capillary number for each specific drop size and offset. According to the simplest picture, as Ca is increased, we would expect the two drops to rotate further prior to coalescence, with the limiting case for $Ca = Ca_c$ occurring when the drops coalesce just at the orientation angle where the flow begins to pull them apart.¹ However, we did not find this result at all. For small viscosity ratios, ≤ 0.1 , coalescence almost always occurred much earlier in the collision process.¹⁰ In particular, the coalescence angle for small and moderate offsets was always nearer the initial collision angle, than to the angle ($\pm 45^\circ$) at which the drops begin to separate, even as Ca approaches Ca_c ! As discussed below, this suggests that the film drainage process (with a time-dependent force along the line of centers as the pair of drops rotate in the flow)

produces a much more complicated evolution of film shapes than anticipated by the simplest models, with the minimum film thickness (or at least the most unstable configuration) occurring much earlier in the collision process. However, there is currently no other direct experimental or theoretical evidence to support this conjecture. For larger viscosity ratios,

> 0.1 , the observations are even more perplexing.¹⁵ Here, for sufficiently small offsets (this depends on the viscosity ratio), coalescence is still observed at small angles for all Ca up to the critical value, Ca_c . However, for larger offsets, the coalescence angle makes a *discontinuous* jump from small angles less

than 45° to angles exceeding 45° as the Ca increases (see Fig 1).

Hence for a range of capillary numbers up to Ca_c and for all but the smallest viscosity ratio drops, there are initial offsets where *coalescence is observed to occur during the portion of the collision process where the force from the external flow is actually pulling the drops apart*. Although some numerical studies have also previously reported coalescence during this portion of the collision process, the proposed mechanism does not seem to be applicable to the current experimental observations.³ On the other hand, a detailed mechanism for these phenomena has not yet been confirmed, either experimentally or theoretically. This is one of the primary objectives of the present proposal, which can be studied in the SFA experiment, as we will explain below.

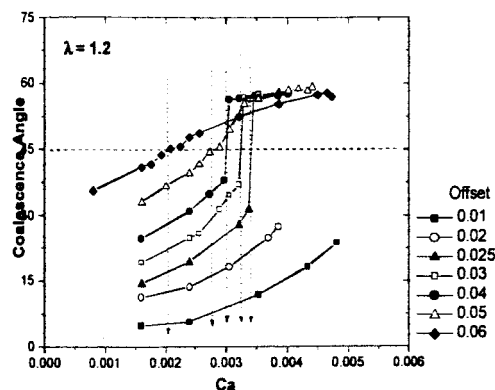


Figure 1. Coalescence angle vs. capillary number for various offsets from head-on collisions. The viscosity ratio was 1.2. Note the discontinuity of the angle at a critical Ca, and coalescence for angles greater than 45° where the drops are being pulled apart by the external flow (from ongoing PhD work of Y. Yoon)

2) Surfactant Effects on the Coalescence Process. We have also carried out, though not yet entirely completed, a study of the effect of an adsorbed surfactant on the coalescence process. In the present experiments, this was done by allowing a di-block ‘copolymer’ of the same molecular species as the two bulk phase fluids to form at the liquid interface. This material is a ‘surfactant’ (i.e., surface-active) for this system, where we can control the equilibrium interface concentration, and also the mobility by modifying the molecular weights of the two components of the copolymer. Details of the experimental protocol are offered in two recent papers.^{9,11}

We observed that the addition of even tiny amounts of ‘surfactant’ at the drop surface is sufficient to strongly inhibit coalescence, in the sense that the critical capillary number is reduced relative to that for drops with a clean interface. In addition, the ‘drainage time’ between initial collision and coalescence in a head-on collision is sharply increased at any given capillary number. In making these comparisons, the equilibrium interfacial tension of the interface with surfactant present was used in calculating the capillary number. We have obtained ‘complete’ data for drops with two different viscosity ratios, 0.19 and 1.2, for a single surfactant entity (i.e., for a single fixed copolymer molecular weight), as a function of the equilibrium surfactant concentration (the latter determined indirectly by measuring the change in the equilibrium interfacial tension relative to that for the clean interface).¹¹ For technical reasons having to do with the use of drop breakup to produce a pair of equally sized drops for use in the coalescence studies, the maximum surfactant coverage was actually fairly low, corresponding to no more than a 15-20% decrease in the interfacial tension. However, for the systems we studied, the majority of the surfactant effect is already present at the lowest surfactant concentrations, for which the equilibrium interfacial tension is decreased by as little as 5%. We believe that the basic mechanism by which this un-charged surfactant inhibits coalescence is that Marangoni stresses within the thin film tend to immobilize the interface and slow the film drainage process. This is plausible, in spite of the slow flows and the low surfactant concentrations, because the coalescence process takes place at very low capillary numbers, meaning that only a very tiny Marangoni contribution to the tangential stress balance in the thin film is sufficient to balance the viscous stresses within the film and thus immobilize the interface. However, a major puzzle from our initial measurements of the changes in the critical capillary number (or drainage time) with surfactant addition was that the inhibition of coalescence for the higher viscosity ratio drops did not increase monotonically with the increase of the surfactant concentration (see Figure 2).

Motivated by this latter finding, Cheng, Cristini and coworkers¹⁶ utilized numerical simulations to discover a mechanism by which a surfactant could first inhibit coalescence and then reverse at higher concentrations. The basic idea is that the capillary number is defined based on the

equilibrium concentration of the surfactant, but that the flow in the thin film might sweep the surfactant out of the film, thus increasing the interfacial tension there and producing film shapes and drainage rates that are comparable to a clean drop at a lower capillary number. This is a simple and clever idea, but we do not believe that it explains the data we have obtained, because the mechanism only becomes significant at much higher surfactant concentrations at the interface than anything we have studied in the

lab. To explore this phenomenon further, we again carried out detailed studies of the droplet trajectories during coalescence. These studies show that the immobilization of the interface due to Marangoni stresses again provides a mechanism for *both* low and high viscosity ratio drops to coalesce at angles in excess of 45° (i.e. when the external flow is already pulling the drops apart).

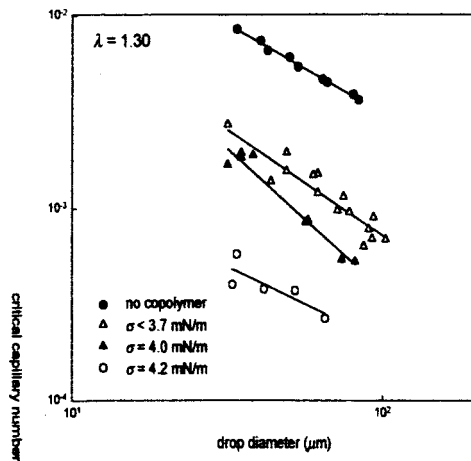
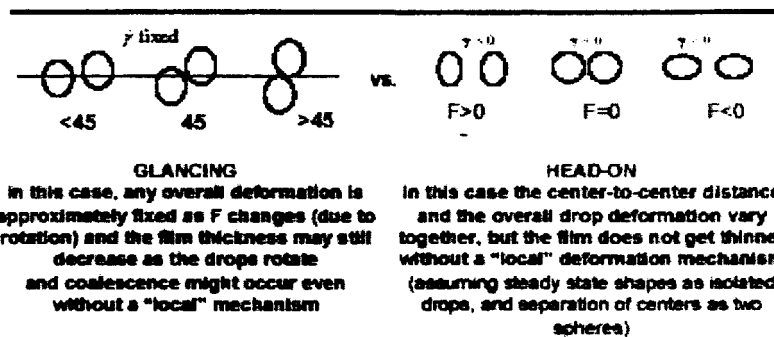


Figure 2. Critical capillary number versus drop size for various levels of surfactant coverage of the interface. Note the lowest surfactant concentration produces the largest decrease in Ca_c and the effect of adding additional surfactant is non-monotonic in surfactant coverage(from paper of Ha et. al ¹¹)

When coalescence occurs at larger angles, there is more time for a film to thin and the critical capillary number is increased. In the case of the higher viscosity ratio drops, the critical coalescence angle increases monotonically with increase in the surfactant concentration, and hence the reduction of the film drainage rate due to Marangoni effects is compensated by the increased drainage time for rotation to larger angles. This causes the critical capillary number to increase at higher coverage levels. For the lower viscosity ratio system, the critical coalescence angle jumps at the lowest surfactant concentrations to approximately 65° , and is then independent of the surfactant concentration. The critical capillary number is larger than one would expect if coalescence were confined to angles smaller than 45° (as expected by simple models), but since coalescence occurs at a fixed angle, Ca_c does decrease monotonically in this case with increased coverage. *Of course, the major unresolved question in these surfactant studies is again the mechanism for coalescence at angles greater than 45° , as well as any relationship with the similar observations at increased offset in the clean interface problem.* The experiments proposed here will address this question.

(3) Head-on Collisions with Time-Dependent Velocity Gradient and No Surfactant. Inherent in the experiments described above are a number of unresolved questions about the details of the mechanisms of film drainage and rupture. Chief among these questions are the evolution of film shapes in glancing collisions that lead to coalescence either early in the collision process, or very late in this process while the drops are being pulled apart by the external flow. In the latter case in particular, the mechanism that leads to *local* thinning of the film at the same time that the centers of the drops are moving apart has at least two possible explanations. One is that the small but fixed overall deformation of the drops leads to thinning as the drops rotate around each other in a flow with fixed velocity gradient. (sketch) Another is that the suction pressures induced in the thin film as the drops are pulled apart



causes a *local* outward deformation that locally reduces the film thickness. Two potential routes to resolving these questions are (i) detailed measurements of the film geometry in the surface forces apparatus (SFA) that constitutes a central part of the present proposal, and (ii) theoretical simulations. However, the most straightforward measurements that can be done in the SFA are *axisymmetric* in a 'head-on' configuration but with a time dependent force along the symmetry axis that mimics the force along line of centers of the two drops rotating in the flow of the 4-roll mill¹⁵. The simplest simulations which can be done with super-high accuracy are also axisymmetric, rather than fully 3D configurations, and one can again simulate the film drainage process with a time-dependent force that decreases in magnitude and eventually changes sign. If the drops remained exactly spherical, their interaction in a flow can be *exactly* decomposed into axisymmetric translation along the line of centers and rotation. However, when the drops deform, this decomposition is no longer precisely correct, and it is not obvious whether the dynamics in an axisymmetric mode (either in the SFA or theoretical) will be a sufficiently good approximation to allow for meaningful comparisons with data for "glancing collisions".

These issues were recently investigated by carrying out head-on collisions in the 4-roll mill, in which two drops were brought together with a time-dependent force induced along their line of centers via time-dependent changes in the magnitude of the velocity gradient produced in turn by time-dependent changes in the cylinder rotation rate (ongoing PhD research of Marcos Borrell). These experiments were carried out with the time-dependent force chosen to mimic the force along the line of centers of a pair of spherical drops that rotate (in a glancing collision) in the same flow. The results in all cases were that coalescence was observed to occur at a

point in time that precisely corresponded to the angle at which coalescence was actually observed in the glancing collision, including cases where coalescence occurred after the force had changed sign (i.e., the direction of rotation of the rollers had reversed after passing through zero). The latter result makes it clear that the mechanism for coalescence beyond 45° in the glancing collisions must be due to 'local' deformation in the thin film rather than being a consequence of global or overall deformation of the drop, because the overall deformation is approximately fixed in the glancing collision (the velocity gradient is fixed) while the overall deformation is time-dependent in the head-on collision with a time-dependent force (i.e., because the velocity gradient in this case is time-dependent). Equally important, these results indicate that the *three-dimensionality* of a glancing collision with deformation does not contribute significantly to the film drainage or rupture process, and thus provides assurance that axisymmetric simulations of this process, either experimentally in the SFA or via axisymmetric flow calculations, will provide relevant information for understanding the 'real' process.

(4) Comparisons with theoretical predictions. Comparisons were made of all of the data from part (1) above with an adaptation of the simple 'scaling' theory for coalescence due to Chesters.¹ For low viscosity ratio systems, the data in the absence of surfactant shows good agreement with expectations from this theoretical model. In particular, for head-on collisions, the measured drainage times between initial 'collision' and coalescence scale with $Ca^{3/2}$ as expected, and the critical capillary number decreases with increase of the drop size, viscosity ratio and offset.

However, in many important respects, the experimental data were at odds with the simple model of Chesters, as well as the qualitative picture of the coalescence process that it represents. First, even when coalescence occurs for angles less than 45° as anticipated by the scaling model, the measured film drainage times (for head-on collisions), the critical capillary number (for 'glancing' collisions), and the *quantitative* dependence on R , θ and the offset is different than predicted. These scaling dependencies are a direct reflection of the dependence of the critical film thickness h_c (or the most unstable film configuration) on R , θ , Ca and offset, and hence on the details of the instability process that leads to film rupture. Another point of strong disagreement is the observed angle for coalescence at the critical capillary number, both for small and large θ . According to the simple picture of the coalescence process, where film thinning is monotonic in time up to the point at which the force along the line of centers changes sign, coalescence at Ca_c should occur in the 4-roll mill at $\pm 45^\circ$. However, for small $\theta \leq 0.1$, the observed 'critical angles' are typically much closer to the initial collision angle, i.e., much smaller, than expected. This can only be interpreted as suggesting that the evolution of film shapes is much more complex than anticipated by the simple model, with the minimum thickness (or the most unstable film configuration) occurring before the pair of drops has rotated very far. This must be a consequence of the fact that the force along the line of centers, tending to push the drops together, *decreases* sharply with time as the drops rotate in the flow. For $\theta > 0.2$, on the other hand, there is a critical offset beyond which there is a discontinuous jump in the coalescence angle with increasing Ca to coalescence angles $> 45^\circ$, where the flow is actually pulling the drops apart. Finally, for surfactants, there is currently no theory that satisfactorily explains the experimental observations that we have made.

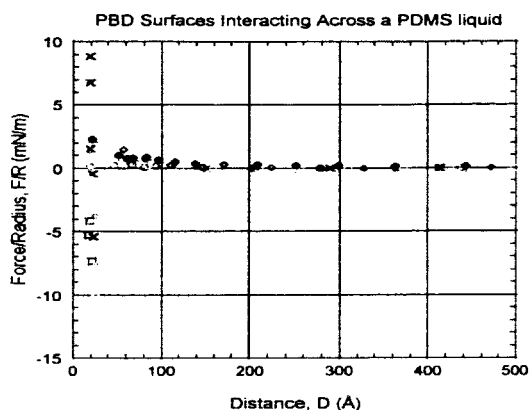
MICRO- AND NANO-SCALE SURFACE FORCES APPARATUS (SFA) STUDIES: SURFACE FORCES AND LOCAL DEFORMATIONS

(1) Measurement and characterization of the attractive van der Waals and hydrophobic forces between liquid-liquid surfaces. One of the most important elements that will be necessary in any successful quantitative theoretical modeling of the coalescence process is the nature and quantitative details of the non-hydrodynamic attractive force across the thin film, which eventually leads to its rupture. For the PB/PDMS polymeric liquids used in the 4-roll mill experiments to date, the dominant attractive force is van der Waals attraction. However, for liquid systems that involve water, water based solutions, or possibly other polar liquids, a stronger and longer range force is the "hydrophobic" force, about which less is known and even the mechanism which produces it is not understood. As we anticipate extension of the macroscopic studies to other liquids (for some of which microgravity will be important as already indicated), we will need detailed data and understanding of the short range non-hydrodynamic forces. This is the natural domain for the SFA, and is one of the main uses we have made of it during our previous NASA sponsored investigation.

(a) Van der Waals forces. Using the SFA, we have measured the van der Waals forces between two curved liquid-liquid interfaces (equivalent to two droplets interacting in a liquid medium). For this system we measured the force between a viscous layer of the polymer polybutadiene (PB) interacting across the polymer

melt, polydimethylsiloxane (PDMS). The results are shown in Figure 3. The measured attractive force at the ‘jump-in’ instability at $D \approx 30 \text{ \AA}$ is in surprisingly good agreement with (1) the Lifshitz theory of van der Waals forces, and (2) also agrees qualitatively with the critical separation distance (i.e., the critical film thickness) (74 \AA) estimated from the critical capillary number in 4-roll mill experiments using a simple scaling theory for the drainage between two equal size drops¹⁰.

Figure 3. Equilibrium force-distance profile for two viscoelastic poly-butadiene (PB or PBD) surfaces in poly-dimethyl-siloxane (PDMS) liquid at 25°C. The attractive van der Waals force causes a ‘jump-in’ instability to occur at a separation of $\sim 30 \text{ \AA}$ from adhesive contact, in good agreement with theory. The depth of the adhesive force, however, is lower than expected when compared to theory or when compared to the known interfacial energy of the PB-PDMS interface. The van der Waals forces are expected to be the same for lower viscosity PB surfaces (e.g., of liquid droplets) interacting in liquid PDMS, as were used in the coalescence studies (described below).



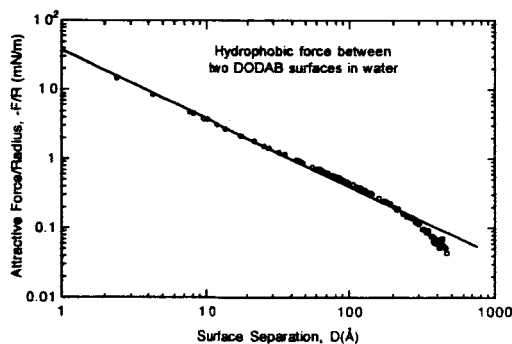
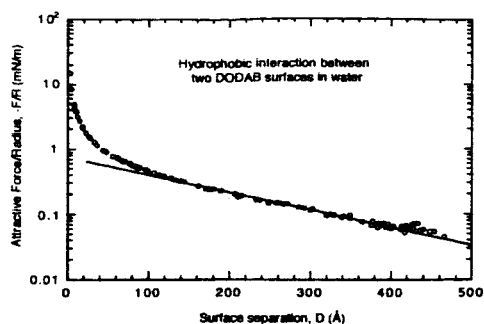
The strength of the adhesive minimum $F/R = -10 \text{ mN/m}$, as measured from the pull-off force, corresponds to an adhesion energy of $F/3\pi R = 1 \text{ mJ/m}^2$. This may be compared with the interfacial energy of the PB-PDMS interface of $\gamma_i = 4 \text{ mJ/m}^2$, which is about 4 times higher than the value measured from the adhesion force. This ‘discrepancy’ is attributed to the oscillatory nature of the ‘solvation’ force between the two relatively rigid PB surfaces interacting across PDMS at short-range.^{17,18} The oscillatory solvation force is known to exhibit secondary adhesive potential energy minima at successive ‘quantized’ separations of periodicity corresponding to the PDMS molecular diameter. These secondary and higher order minima are generally a factor of e, e^2, \dots , etc., weaker than the ‘primary’ minimum at true PB-PB contact. Such short-range oscillatory forces do not arise between less viscous, more fluid-like surfaces (for example, between PB of lower MW which was used in our studies of liquid-liquid coalescence, as described below) because they do not present a *hard* boundary that is required to order the solvent (PDMS) molecules into quasi-crystalline layers that act as repulsive barriers.

(b) Hydrophobic interactions. Early on in this project we constructed a new SFA chamber allowing for hydrophobic and other colloidal interactions to be measured at high temperatures (strictly, over a range of temperatures from 20 to 100°C) under highly stable conditions, i.e., with minimal drift between the surfaces. We also introduced a high-speed camera for recording the optical interference (FECO) fringes that provide direct visualization of the surfaces in *real time*, and measurement of their local shape and separation (to 1-10 Å).

Using this new apparatus and high-speed camera we have, for the first time, accurately measured the hydrophobic interaction between two hydrophobic surfaces over the complete distance regime, especially in the previously inaccessible regime from $D = 50 \text{ \AA}$ down to contact at $D = 0$. The absence of hard data of this kind has led to much speculation about the origin and nature of this important interaction. Our first conclusion is that the ‘long-range’ hydrophobic interaction is almost certainly *not* due to the Laplace pressure force arising from previously existing micro-air bubbles or water-vapor cavities bridging two approaching hydrophobic surfaces. We see no discontinuities in the FECO fringes (which can also be used to measure refractive index changes to

0.01) as the two surfaces accelerate into contact, nor any discontinuities in the force-distance curves (see Figure 4) that would be expected if a liquid-vapor phase separation of vapor cavities were occurring between the surfaces. Neither are our results ‘statistical’, but highly reproducible: some previous AFM measurements¹⁹ have found large variations in the range of the measured forces and concluded that this must be due to the presence of randomly-sized air bubbles on the surfaces.* Our finding therefore rules out one of the current models of the hydrophobic interaction.

* Two recent theories²² suggest that time-dependent density fluctuation in the water film between two approaching hydrophobic surfaces (analogous to the statistical nature of any nucleation process) may be important in



(a)

(b)

Figure 4. (a) Measured hydrophobic force F versus distance D between two crossed cylindrical curved surfaces of radius R coated with a surfactant layer of DODAB in water at 25°C. The straight line indicates that the force is exponentially attractive at distances greater than ~10 nm, as previously found for other hydrophobic systems. (b) Same results as in (a) but plotted on a log-log graph. The straight line has a slope of -1 which indicates that the force is inversely proportional to D at distances below ~10 nm. These are the first data of hydrophobic forces at separations below 5 nm, which were obtained using a high-speed camera to monitor the surface separation as the two surfaces rapidly ‘jumped’ into adhesive contact as a consequence of the attractive (hydrophobic) force between them.

Our second important finding is that the force, shown in Fig. 4(a) on a semi-log plot and in Fig. 4(b) on a log-log plot, is exponential at large separations, above 10 nm, as previously reported by many authors, but changes to a power law at small separations. The exponent of the distance dependence is -1.0 which implies a force (between two curved surfaces) that goes as $F = \text{Const}/D$, which may be compared with $F = \text{Const}/D^2$ for the van der Waals force. We have no theoretical explanation for the observed distance dependence, but our current priorities are anyway to first establish whether this result is general. Thus, our work is continuing with different hydrophobic surfaces (both solid and fluid) at different temperatures, at different approach rates, in different electrolyte conditions, etc., which may soon allow us to provide the answer to this important question.

(2) Surface deformations on approach and coalescence of two fluid-fluid interfaces. The optical technique used in SFA experiments employs interference fringes known as ‘fringes of equal chromatic order’ or FECO²⁰ to visualize two approaching surfaces or interfaces while measuring their separation and deformations in *real time* at the nano-scale (the normal resolution is ~1 Å, the lateral resolution is ~1 μm). Initial proof of concept

determining the hydrophobic force. The time-dependence of these fluctuations is expected to depend on the size or area of the interacting surfaces. If so, then stochastic data in force measurements involving small areas of interaction, as occurs in AFM experiments, is to be expected, but not in SFA experiments where the effective area of interaction area is large.

experiments were carried out using the standard SFA protocol of a fixed approach velocity and the standard crossed-cylinder, non-axisymmetric geometry. Both qualitative and quantitative information were obtained on the different types of surface deformations that can occur prior to contact (coalescence), the coalescence process itself, and the subsequent growth of the coalesced region. Figure 5 shows the generic geometry of two approaching liquid-liquid layers, showing the parameters that can be directly measured and/or controlled during these experiments, although so far, as described in Fig. 3 above and further below, only a limited number of quantitative results have been obtained, and these on non-axisymmetric surfaces.

Figure 5. Surface geometry in SFA experiments used to measure the forces and deformations of two approaching liquid-liquid interfaces. The directly measurable and/or controllable parameters as a function of time t are: the approach velocity V , the hydrodynamic or intermolecular force $F(D)$, and the interface shape or profile $D(r)$ such as the local radius of curvature of the two PBD-PDMS interfaces interacting in PDMS. When necessary, one can also measure the refractive index of the different media. The viscosity of PBD can be varied over a large range by varying the molecular weight, which has only a small effect on its surface tension, refractive index and van der Waals forces (Hamaker Constants) across different media.

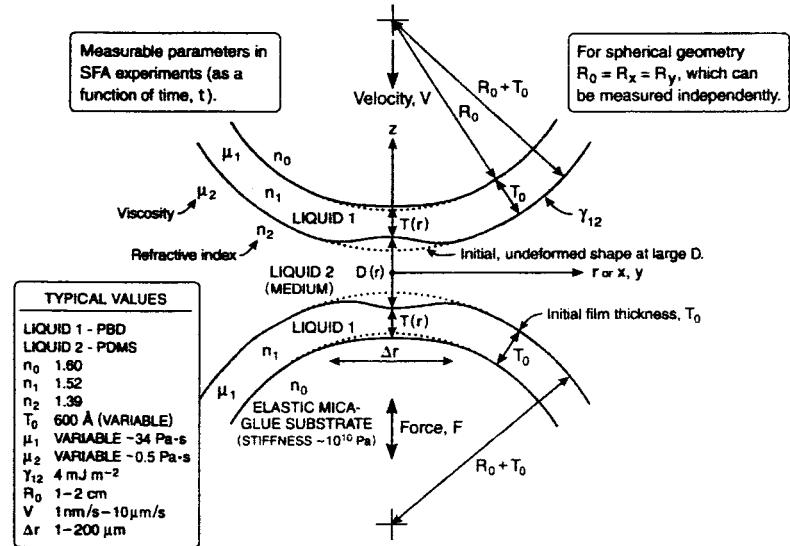
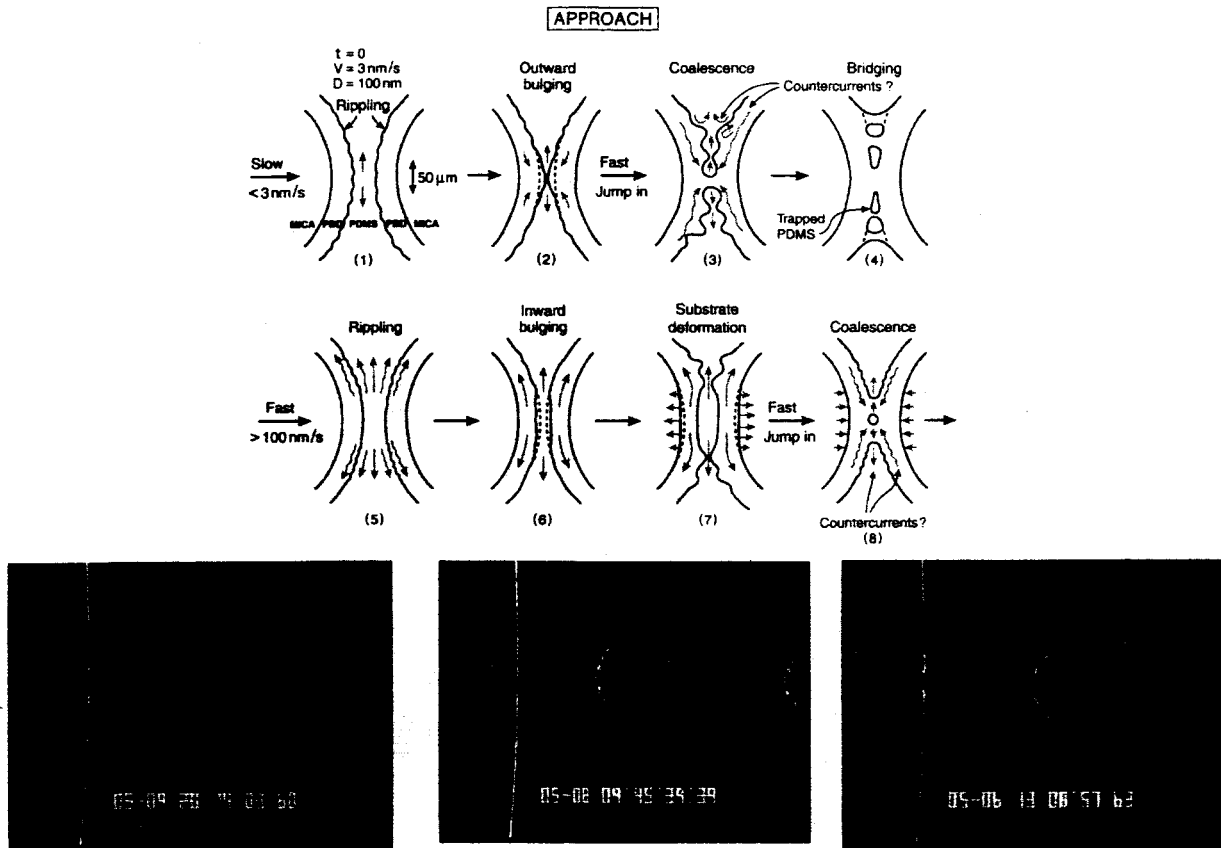


Figure 6 shows the complex shape changes that occur during the approach and coalescence of two fluid-fluid interfaces. These depend on the approach velocity V , the fluid viscosities, μ_1 and μ_2 , the initial surface radii R_0 , and the intermolecular forces between the two interfaces $F(D)$. These results reveal a very complex series of processes occurring either simultaneously or sequentially at different length and time scales. Correlating the occurrence of coalescence and the film deformation process leading up to it with the macroscopic system (4-roll mill) observations, for spherical rather than non-axisymmetric crossed-cylinder surfaces, forms the basis of the proposed SFA experiments and theoretical modeling described in Part III. Suffice it to say here that the thin film dynamics under the constant approach velocity conditions of the standard SFA configuration is qualitatively interesting, but not directly comparable to the conditions for film deformation and thinning in the 4-roll mill flow-induced coalescence experiments. In the latter case, the film dynamics occurs under conditions of either constant force (in the case of a head-on collision), or a time-dependent and monotonically decreasing force in all other cases where the two-drop pair rotates in the flow during the collision process. The work we (and others) have done to date has focused us on the fact that the film dynamics is much more complex than we had originally imagined and that it is also essential to repeat (and expand) the experiments to incorporate controlled forces rather than only controlled normal velocity conditions.

Quantitative results in air: During the initial stages of our research, in order to ‘get a feel’ for what to expect, we first studied the coalescence of liquids in air where the large refractive index difference allowed for greater accuracy in measuring liquid surface profile changes and surface-surface separations. In such situations the viscosity of the medium, i.e., air, is negligible and we found that as two (curved) liquid surfaces were made to slowly approach each other they deformed by bulging towards each other before coalescing. This ‘outward’ bulging is due to the attractive long-range van der Waals forces between them. The slower the approach the greater was the bulging, since it required the flow of liquid from the thin film into the interaction zone.



FECO fringe pattern of two approaching but as yet undeformed liquid surfaces.

FECO pattern showing surface ripples (waves) as shown schematically in (1) above.

Refractive index discontinuity of coalesced surfaces as shown schematically in (8) above.

Figure 6. Surface deformations during the approach and coalescence of two crossed cylindrical curved surfaces ($R=1$ cm) of liquid PB ($\mu_1=34$ Pa s) in liquid PDMS ($\mu_2=0.5$ Pa s) as visualized in SFA experiments using both multiple beam interference FECO fringes (lower panels) and standard optical microscopy. Top row of top panel: slow approach ($V < 3$ nm/s). Bottom row of top panel: fast approach ($V > 100$ nm/s). At low approach rates, hydrodynamic deformations are small and the interfaces bulge *towards* each other before coalescing due to the attractive van der Waals force between them, as described in Fig 3. At high approach rates hydrodynamic forces dominate and give rise to an inverted dimple before contact, i.e., the two surfaces bulge *away* from each other. Just before and immediately after coalescence, ripples and multiple contacts can often be seen fanning out from the central neck region. These crossed-cylinder experiments need to be repeated for the sphere-on-sphere geometry, as proposed in Part III.

For two surfaces of initial (undeformed cylindrical) radii $R=2$ cm each supporting a PDMS film of thickness $T_0 \approx 100 \text{ \AA}$ (see Fig. 5), the maximum bulging was found to be $\sim 1,000 \text{ \AA}$ before the surfaces coalesced (Fig. 7a). Theoretically, the van der Waals interaction force between two crossed-cylinders each of radius R (the SFA geometry, which at small surface separations D is equivalent to two equal spheres of radius $2R$ at the same separation)¹⁸ is given by $F = \frac{A}{D^2}$, where A is the Hamaker Constant. Under equilibrium conditions, e.g., during slow approach, a point of instability is expected to occur at a separation D_j from which the surfaces spontaneously 'jump' into contact and coalesce. This instability condition is given by $\frac{A}{D_j^2} = K$, where K is the effective spring constant or stiffness of the supporting spring or substrate (in units of N/m). Now, when K is determined by the energy or force needed to bulge a liquid surface, it can be shown²¹ that $K = \frac{2\gamma}{R}$ where γ is the surface (or interfacial) tension of the liquid-vapor (or liquid-liquid) interface. For our

PDMS film coalescence experiments in air, we have $\gamma = 40$ mN/m, $A = 5 \times 10^{-20}$ J, $R = 0.02$ m, so that we expect (theoretically): $D_j \approx 1,000$ Å, where D_j is measured relative to the *undeformed* surfaces. This is a very large value, but of the same order as the value measured for the bulging of two PDMS surfaces, as shown in Fig. 7(a).

Quantitative results in a liquid medium: Similar effects were expected to occur for liquid PB films interacting across PDMS except that now (i) the Hamaker Constant is lower (cf. Fig. 3), (ii) the interfacial tension is lower ($\gamma = 4$ mN/m), and (iii) the viscosity of the intervening liquid medium can no longer be ignored except at extremely low approach velocities. Figure 7(b) shows our preliminary results for two PB films approaching each other in PDMS²². Under these conditions, the PB surfaces bulge *inwards*, as was illustrated schematically in Figs 5 and 6, because the viscous forces now dominate over the attractive van der Waals forces. The results of Fig. 7(b) reveal a complex time evolution of both the shapes of and separation between the two liquid-liquid interfaces as they come together. As proposed in Part III, more experiments over a large range of variables are needed before a complete and quantitative picture is obtained that would allow for detailed theoretical modeling.

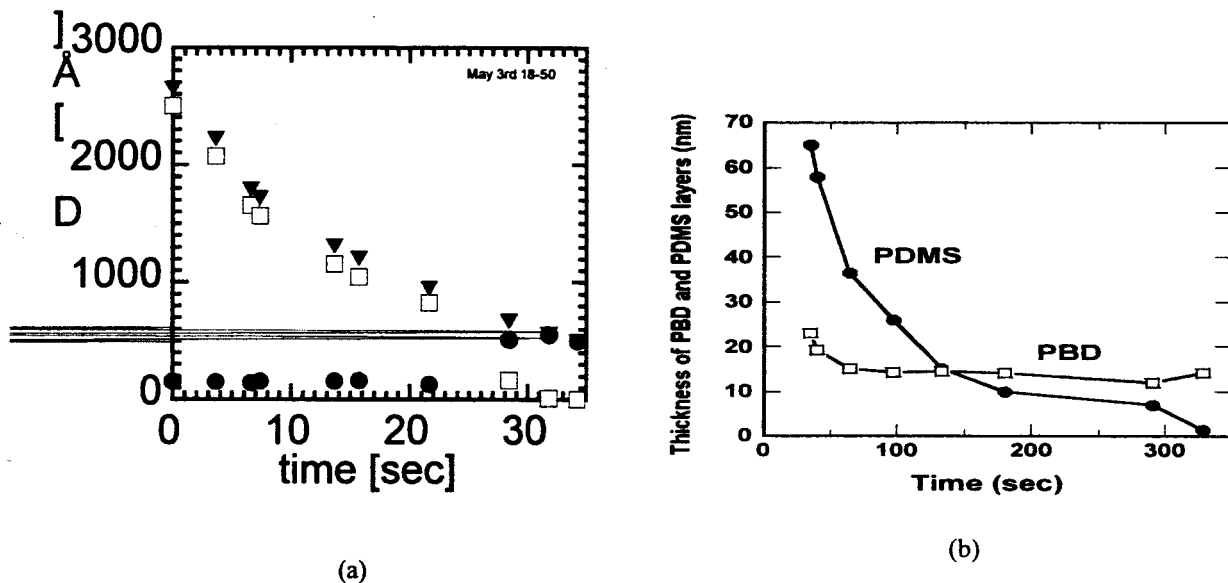


Figure 5. (a) Two PDMS surfaces approaching in air. Black triangles: Total separation between supporting mica substrate surfaces. Squares: separation between liquid surfaces. Blue points: PDMS film thickness. Coalescence occurs at $t = 30$ sec. (b) Two liquid PBD surfaces approaching across PDMS. The ‘intervening’ PDMS film thickness falls progressively as it drains out, slowing down due to viscous drag, but finally accelerating to zero thickness as the van der Waals force finally pulls the two interfaces together at $t = 300$ sec. Each PBD film also initially thins, but finally increases (bulges out, as in (a)) as the van der Waals force pulls the two PBD-PDMS interfaces together.

(3) Studies of liquid coalescence and detachment under true thermodynamic equilibrium conditions (as distinguished from ‘mechanical’ instabilities). As explained above, we initially studied the coalescence of liquids in air, i.e., exposed to or surrounded by vapor rather than immersed in another liquid medium. We quickly realized that the conditions of *constant liquid volume* are not thermodynamic, and that under true thermodynamic equilibrium conditions it is the *chemical potential* that remains constant during the coalescence and detachment processes, which are (indeed, must be) reversible. For a liquid, especially a ‘volatile’ liquid, exposed to its own vapor this means that molecules are continually being exchanged between the liquid and the vapor ‘reservoir’, i.e., that their volume continually changes, during both of these processes. Our results²³ with more volatile liquids such as cyclohexane and low MW alkanes show that the whole process is then very different from that occurring between ‘involatile’ liquids or droplets (such as PBD and PDMS) whose volumes can be assumed to remain constant during coalescence. However, even for volatile liquids, under conditions of

rapid approach (or separation) the constant volume conditions do appear to hold even at the sub-microscopic scale, as was established quantitatively for rupturing liquid necks of dodecane and hexadecane²⁴

RECENT PUBLICATIONS RELEVANT TO THIS PROJECT

- (1) **Experimental Trajectories of Two Drops in Planar Extensional Flow**, D.C. Tretheway, M. Muraoka, and L. G. Leal, *Physics of Fluids*, **11**, 971 (1999).
- (2) **A Note on Drop Deformation Breakup and Coalescence with Compatibilizer**, Y. T. Hu, D. J. Pine and L. Gary Leal, *Physics of Fluids* **12**, 484 (2000).
- (3) **The Coalescence of Two Equal-Sized Drops in a Two-Dimensional Linear Flow**, H. Yang, C. C. Park, Y. T. Hu and L. G. Leal, *Physics of Fluids* **13**, 1087 (2001).
- (4) **An Experimental Study of Drop Deformation and Breakup in Extensional Flow at High Capillary Number**, J. W. Ha and L. G. Leal, *Physics of Fluids* **13**, 1568 (2001).
- (5) **Deformation and Relaxation of Newtonian Drops in Planar Extensional Flows of a Boger Fluid**, D.C. Tretheway and L. G. Leal, *J. non-Newtonian Fluid Mechanics* **99**, 81 (2001).
- (6) **Hydrodynamic Interaction Between Spheres Coated with Deformable Thin Liquid Films**, S.M. Yang, L.G. Leal, and Y.S. Kim, *J. Colloid and Interface Sci.* **250**, 457 (2002)
- (7) **The Effect of Compatibilizer on the Coalescence of Two Drops in Flow**, J. W. Ha, Y. Yoon and L. G. Leal, *Physics of Fluids* (in press) (2002)
- (8) **Experimental Study of Molecular Weight Effects on Coalescence: Interface Slip Layer**, C.C. Park and L. G. Leal, *J. Rheology* (submitted) (2002)
- (9) **Mechanism of evaporation, condensation and nucleation in confined geometries**, Nobuo Maeda, Jacob Israelachvili. *J. Phys. Chem.* **106** (2002) 3534-3537.
- (10) **Evaporation and instabilities of microscopic capillary bridges**. Nobuo Maeda, Jacob N. Israelachvili, Mika M. Kohonen. Submitted to *PNAS*.
- (11) **Adhesion and coalescence of ductile metal surfaces and nano-particles**. Norma Alcantar, Chad Park, Jian-Mei Pan, Jacob Israelachvili. *Acta metalia.* **00** (2002) 000-000 (in press).
- (12) **Surface Force Measurements and Nano-scale Visualization of the Deformation, Coalescence and Detachment of Fluid-fluid Interfaces**. T. Kuhl, R. Tadmor, N. Chen, Q. Lin, J. Israelachvili (MS in prep).
- (13) **New Surface Forces Apparatus for Measuring Weak Surface Interactions Under Equilibrium Constant Force Conditions**. Jacob Israelachvili (MS in prep. for *Rev. of Scientific Instruments*).